

# Transient behaviour of quantum-dot saturable absorber mirrors at varying excitation fluence

Niels Meiser · Saulius Marcinkevicius ·  
Valdas Pasiskevicius

Received: 15 October 2013 / Accepted: 23 January 2014 / Published online: 4 February 2014  
© Springer-Verlag Berlin Heidelberg 2014

**Abstract** We present results from studying the carrier dynamics in self-assembled InAs/GaAs quantum-dot saturable absorbers intended for mode-locking of solid-state lasers. Four samples are examined, featuring controlled variations in the resonance condition of the electric field inside the absorber, the number of quantum-dot (QD) layers and the thickness of the GaAs barriers between these QD layers. Pump-probe experiments are conducted at a wide range of excitation fluences and reveal a fast relaxation component of the initial bleaching at low excitation fluences, while a slowly relaxing induced transparency becomes dominant at higher excitation fluences. Time-resolved photoluminescence measurements reveal a large and slowly relaxing induced transparency due to a capture of excess carriers from the barrier bands into the QDs and a slow radiative recombination there. The resonance condition as well as the thickness of the barriers between the QD layers can be used to control the relaxation behaviour. The fastest response is obtained in a structure with an increased number of QD layers at each individual anti-node of the electric field, which is attributed to the appearance of efficient non-radiative recombination channels and capture centres. These centres are probably related to dislocations and other defects appearing in thick QD stacks.

## 1 Introduction

Self-assembled semiconductor quantum dots (QD) deposited by exploiting Stranski–Krastanov growth on lattice-mismatched substrates have been extensively studied over the pasty 20 years, primarily with the aim of realising low-current density threshold laser diodes with concomitantly low sensitivity to operational temperature. Such emitters have been successfully realised (for a recent review [1]) and are now commercially available. The characteristic  $\delta$ -like density of states in QDs can also be beneficial for saturable absorbers used for passive mode-locking of lasers. Specifically, QDs offer inherently low saturation fluence and inhomogeneously broadened absorption spectrum, the latter being due to the non-uniformity of the QD size. Both of these properties are beneficial for mode-locking of high-repetition rate ultra-short-pulse lasers [2–8]. In contrast to the long non-radiative lifetime requirement for light emitters, however, the saturable absorbers for mode-locking should have a fast relaxation of the excited electron–hole pairs, typically of the order of 1 ps, which is beneficial for self-starting mode-locking and pulse stabilisation [9]. In semiconductor saturable absorber mirrors using quantum wells, the absorption recovery is governed by subpicosecond intraband relaxation of excited electrons followed by recombination on the timescale of a few picoseconds [10]. The recombination time in such structures can be reduced by several means, such as low temperature growth or ion implantation, thereby producing a controlled concentration of non-radiative recombination centres. Due to the absence of dispersion in QD electron and hole states, the carrier cooling mechanism cannot be exploited. Therefore, the recovery of the absorption in a QD modulator is governed by the recombination processes. Now, the

---

N. Meiser (✉) · V. Pasiskevicius  
Laser Physics, KTH – School of Engineering Sciences,  
10691 Stockholm, Sweden  
e-mail: nm@laserphysics.kth.se

S. Marcinkevicius  
Department of Materials and Nanophysics, KTH Royal Institute  
of Technology, Electrum 229, 16440 Kista, Sweden

lifetime of the electrons in the ground state of InAs/GaAs QDs with transitions in the 1- $\mu\text{m}$ -wavelength region has been shown to be of the order of several hundreds of picoseconds [11]. Although the electron relaxation from excited QD states has been shown to happen by an order of magnitude faster, on the scale of tens of picoseconds [12, 13], the recovery of a saturable absorber intended for mode-locking broadband gain will eventually be determined by the ground state depopulation. Therefore, for self-starting and stable passive mode-locking and to generate short pulses, the recombination time has to be reduced significantly.

Saturation in QD absorbers obviously relies on QD state filling. The excited electrons and holes then can be further promoted into the 2D conduction and valence bands of a wetting layer (WL) and eventually into the quasi-continuum of states in a GaAs barrier. It has been demonstrated that such excited carrier exchange processes mediated by thermal emission and Auger processes are very efficient and occur on a timescale of a few picoseconds [14–16], i.e., it is about an order of magnitude faster than the fastest relaxation within the QD. The excess carriers in the WL and barrier states can be readily created by electron and hole emission from the QDs, as well as by two-photon absorption from the ultrashort pulse. Due to the efficient carrier capture process from the WL and GaAs barrier bands into the QD states, one can expect a strong dependence of the absorption dynamics on excitation fluence in QD saturable absorber structures. Moreover, it can be expected that the dynamics would depend strongly on the structure design, in particular, the thickness of the GaAs barriers between InAs QD layers as well as the number of QD layers.

In this picture, the various wetting layers and barriers serve as excited carrier reservoirs feeding into the QD states. Therefore, one strategy of increasing the absorption recovery time in QD saturable absorbers, then, is introducing efficient non-radiative recombination centres in the barrier layers either by proton irradiation [17], lower temperature GaAs growth, excess carrier removal by applying a DC bias field [18] or, as in this work, by exploiting strain-induced defects. In the work presented here, we study the excitation intensity-dependent, time-resolved differential reflectivity and the time-resolved photoluminescence (PL) spectra in QD saturable absorber mirror (QD-SAM) structures where designs varied the barrier thickness, the number of QD layers and the resonance conditions for the internal electric field. All structures were grown in the same MBE machine in analogous conditions, had a good optical quality, low saturation fluence (below  $10 \mu\text{J}/\text{cm}^2$ ), but, as it will be shown, the dynamics varied quite drastically.

## 2 Sample description and experimental methods

The samples used in this experiment were grown by molecular beam epitaxy under the same growth conditions, although obviously during separate growth runs. The refractive index profile and the normalised electric field amplitude distributions in two of the QD-SAM samples are shown in Fig. 1. The QD-SAM structure is arranged as follows: first, a highly reflective Bragg stack made of 30  $\text{Al}_{0.9}\text{Ga}_{0.1}\text{As}/\text{GaAs}$  pairs was grown on a GaAs substrate. Self-assembled InGaAs quantum-dot layers (each formed from 1.2 monolayer of InGaAs) separated by GaAs spacer layers follow on top of the high reflector. The QD density in each layer is on the order of  $4 \times 10^9 \text{ cm}^{-2}$ . The QD layers were organised in groups of three (structures A, B, F) or five (structure H), and several such groups were placed at subsequent anti-nodes of the electric field distribution in the sample. A more detailed picture of the QD layers and groups is shown in Fig. 1, while the description of the samples is provided in Table 1. The enhancement factors in Table 1 represent the standing wave electric field amplitude normalised to that of the impinging field and based on theoretical calculation at the vacuum wavelength of 1,042 nm using structure designs. For clarification, Fig. 2 shows the enhancement factor at the first QD stack as a function of wavelength for all of the samples. It also has to be noted that the FWHM spectral bandwidth of the laser used for characterisation was about 7.5 nm. So, the sample A is a resonant one, while structures F, and H are anti-resonant, while the structure B which had a specially designed top layer structure is weakly resonant. It has to be noted, though, that the field enhancement factor is potentially subject to growth errors [19]. The total number of the QD layers and the field strength inside the structure determines the eventual modulation depth. Importantly, the structure H had five QD layers separated by 20 nm in each of three groups. The similar anti-resonant structure F with the same number of QD layers and the same layer separation as in the sample H had five groups of QD layers with three QD layers in each group. For comparison, the structures A and B had similar total number of QD layers but only three QD layers separated by 10 nm per each group. Studying these structures allows obtaining information on the influence of the intra-structure field strength, QD interlayer proximity and the number of stacked QD layers on the absorption relaxation dynamics.

The non-linear reflectivity was measured as a differential signal in a non-collinear cross-polarised pump-probe experiment. The laser used for excitation had a pulse width of 160 fs, a repetition rate of 40 MHz and the spectrum is centred at 1,042 nm (Origami by OneFive GmbH). The laser pulse-to-pulse amplitude stability was better than

**Fig. 1** Field enhancement factor and refractive index profile of the two structures (a) *A* and (b) *F*. The anti-resonant design of sample *F* is immediately recognised. It can also be seen that sample *A* contains one additional group of three QD layers

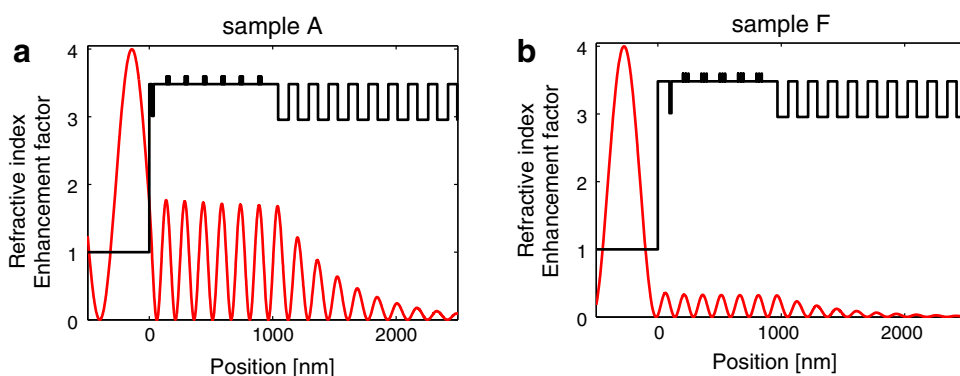


**Table 1** Parameters for the four samples under examination

Sample name	Total number of QD layers	Number of stacks	Number of layers per stack	Spacing inside a stack (nm)	Field enhancement factor at 1,042 nm
A	18	6	3	10	1.59
B	18	6	3	10	1.97
F	15	5	3	20	0.31
H	15	3	5	20	0.58

The field enhancement factor was calculated for a wavelength of 1,042 nm using the transfer-matrix formalism applied to the known designs (see also Fig. 2). The given number is the value of the first maximum inside the structure

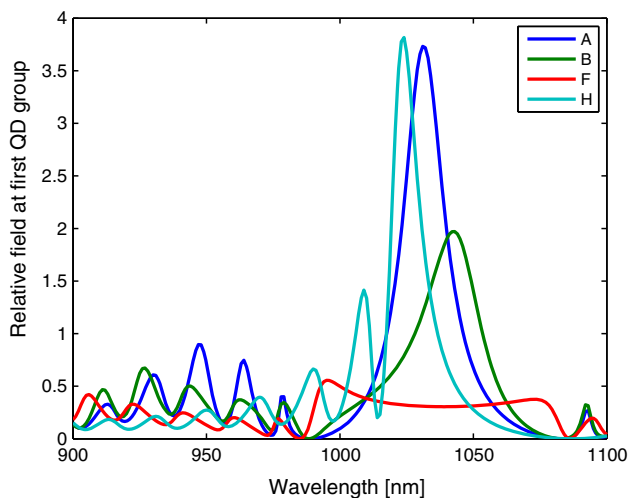


**Fig. 2** Field enhancement factor as a function of the wavelength for all of the four samples. Samples *A* and *H* feature a maximum field enhancement around 1,030 nm, while sample *B* is only weakly resonant, and sample *F* is entirely anti-resonant

0.1 %. The probe beam was split from the main beam by a combination of a half-wave plate and a wedged glass plate at Brewster’s angle. Since the pump beam was not completely linearly polarised, some artefacts were expected around zero delay. However, this effect was weakened by the non-collinear geometry. The pump beam was mechanically chopped at a frequency of 400 Hz. The reflected probe beam was directed towards a photodiode

and the signal was extracted via a regular lock-in detection. Such an arrangement reduces significantly the influence of scattered pump background picked up by the detection system. For each pump fluence, the probe transient reflectivity was recorded as a function of pump-probe delay time with the maximum delay being 25 ps. This measurement produced 2D differential reflectivity maps as those shown in Fig. 3.

In order to investigate the excess carrier capture dynamics from GaAs barriers and WLs as well as the dynamics of the electron–hole pairs in the QDs, we used time-resolved PL spectral measurements. These measurements also offered the possibility to observe the state dynamics over time spans of 1.5 ns. For these measurements, the samples were excited by pulses from a mode-locked Ti: sapphire laser centred at 782 nm (1.585 eV) with the duration of 130 fs (Tsunami by Spectra Physics). The laser beam was focused to the sample with a microscope objective; the luminescence was collected with the same objective and directed towards a grating spectrometer via a beam splitter. Considering that the laser pulse duration is >100 fs and the microscope objective consists of a few millimetres of glass, any pulse broadening by dispersion from the microscope objective is assumed to be small. Residual excitation laser light was filtered by an RG low-pass filter with the cut-on edge at 850 nm. A streak camera synchronised to the laser’s repetition rate (76 MHz) was used for recording the PL spectra as a function of time.

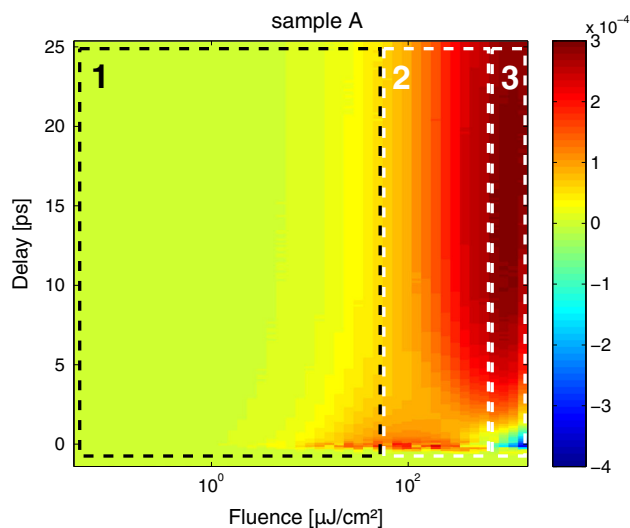


**Fig. 3** Differential reflectivity as a function of the pump-pulse fluence (x axis, logarithmic) and the pump-probe delay (y axis) for sample A. The colour shows the signal from the lock-in amplifier, which is directly proportional to the differential reflectivity. The rectangles mark the regions as mentioned in the text

### 3 Results and discussion

Figure 3 shows the differential reflectivity of the sample A as a function of the pump-probe delay and the excitation fluence. The map for sample A was chosen as an example due to the fact that this structure has the largest field enhancement factor and therefore the largest maximum excess carrier concentration generated at the same input power. The behaviour along the time axis is characterised by the fast relaxation response of the absorber immediately after the excitation ( $\Delta t < 2$  ps) and carrier exchange dynamics between the QDs and the surrounding barrier and WL on longer timescales. The reflectivity maps can be rather arbitrarily subdivided into three pump fluence regions, marked on Fig. 3, where the dynamics has distinct and characteristic traits. In Region 1, corresponding to low fluence, the transient behaviour follows a regular double exponential decay. At higher fluencies, Region 2, the initial incomplete relaxation of the bleached absorption is followed again, after few picoseconds, by an increase in transparency or persistent induced transparency plateau which lasts for durations longer than the 25-ps-scan range in this experiment. At still higher fluencies, Region 3, a new feature of two-photon absorption (TPA) transient appears close to zero delay. Clearly, at which fluence the particular behaviour occurs depends on the internal field strength. For instance, in the non-resonant structures, F and H, the electric field amplitude inside the structure is about an order of magnitude smaller than in the structure A, and the above-mentioned TPA transient was not observed in the range of available pump intensities. In fact, the

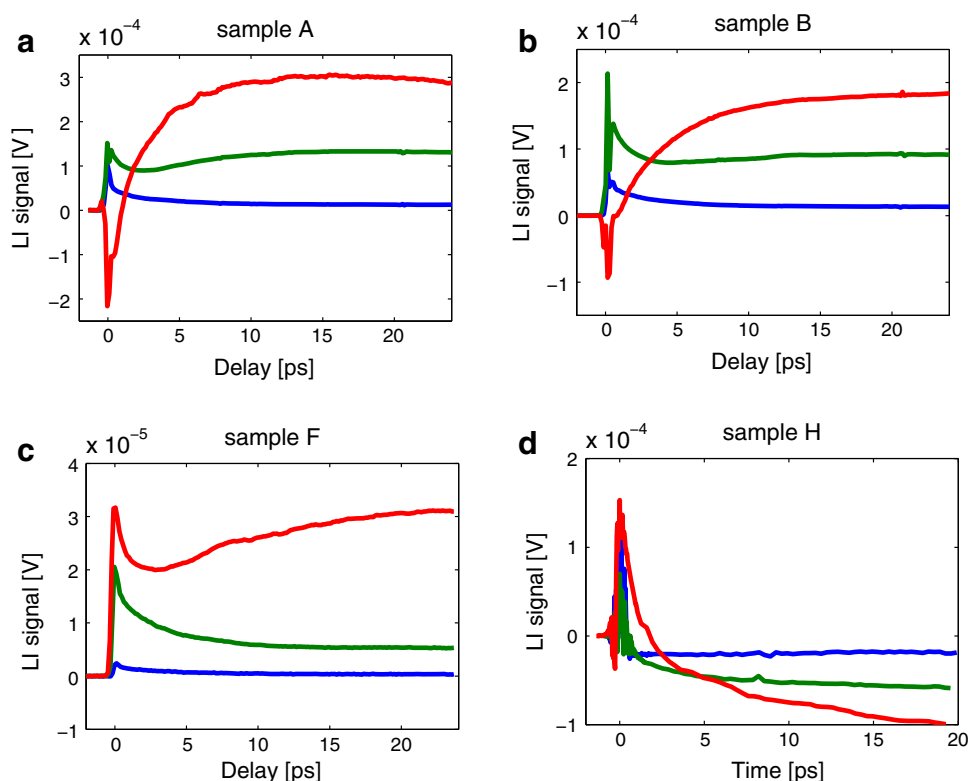
influence of TPA on the reflectivity is well known from absorbers based on quantum wells and is considered important for the stabilisation of mode-locked laser operation [20–22]. Also, the transient response of highly excited quantum well saturable absorbers has been studied and induced absorption as well as a delayed bleaching by the relaxation of TPA generated carriers in the barrier material has been observed [23, 24]. However, similarly, thorough studies of the transient non-linear reflectivity in QDs are, to our knowledge, missing, although the same behaviour has been observed, and carrier capture by QDs has been suggested [25, 26].

The traces of differential reflectivity dynamics at low, medium and high fluencies, extracted from the maps as in Fig. 3, are shown in Fig. 4. At low pump fluencies, the structures A, B and F show an absorption recovery that could be fit by a sum of exponential functions  $a\exp(-t/\tau_f) + b\exp(-t/\tau_s)$ , where  $\tau_f$ ,  $\tau_s$  denote the time constants of fast and slow decay, respectively. The fast time constant is in the subpicosecond range, while the slow component varies between 3 and 4 ps in the above-mentioned three structures (A, B and F). The eventual dynamics is determined by the ratio of the amplitudes  $a/b$ , which is smallest in the resonant structure A, and is 2–3 times larger in structures B and F. At higher pump fluencies of about  $140 \mu\text{J}/\text{cm}^2$  in samples A, and B and  $720 \mu\text{J}/\text{cm}^2$  in the non-resonant sample F, the initial fast relaxation of the transparency is followed after about 3 ps by the transparency rising again and staying high for durations longer than 25 ps.

At still higher pump fluencies, in structure A and to a smaller extent in the structure B, the two-photon absorption appears as an initial short dip in reflectivity, followed by an increase in transparency that persists for durations longer than 25 ps. The polarity reversal is similar in the structure B, however, the TPA dip is smaller at the same pump fluencies, which is consistent with the generally smaller field enhancement factor in the structure B. In contrast, the non-resonant structures F and H do not exhibit an initial increase in absorption up to the fluencies of  $720 \mu\text{J}/\text{cm}^2$  owing to the lower internal field strength. The slow relaxation component as well as the delayed decrease in absorption at higher excitation densities in structures A, B and F can be attributed to the process of recapture of the excited carriers from the wetting layer and the barrier states. In high crystalline quality structures with a low concentration of non-radiative defects in the barriers, such pools of excess carriers can be long living. For the purposes of applications of such structures for laser mode-locking, such dynamics is not desirable.

In the structure H, however, the differential reflectivity dynamics is quite different. At low intensities, the induced transparency relaxes within 0.5 ps. The measurement is

**Fig. 4** Differential reflectivity as a function of the pump-probe delay from samples (a) A, (b) B, (c) F and (d) H at three different excitation fluences (blue line 12  $\mu\text{J}/\text{cm}^2$ , green line 140  $\mu\text{J}/\text{cm}^2$ , red line 720  $\mu\text{J}/\text{cm}^2$ ). Note the different order of magnitude on the y axis in graph (c) for the anti-resonant sample F



limited here essentially by the resolution of the set-up. At higher intensities of 140 and 720  $\mu\text{J}/\text{cm}^2$ , the initial fast relaxation is followed by induced absorption. The differential reflectivity dynamics in this sample is determined by a very efficient channel that removes excited carriers from the QD states. Such channel might be captured by defect states in the barriers which, when filled, would give rise to additional absorption by transition into the quasi-continuum of WL and/or barrier states. Note that, the structure H contains the same total number of QD layers (15) as the structure F, and the distances between the QD stacks are the same; however, in the structure H, there are five QD layers per stack as compared to three layers in the structure F. A larger number of InAs QD stacks with 25-nm spacer layer have been shown to generate non-radiative defects due to accumulated stress in the stack [27, 28]. In any case, the differential reflectivity dynamics in sample H is that of a fast saturable absorber, and the induced absorption following the initial transparency peak is beneficial for the stabilisation of mode-locking operation. Indeed, structures as in sample H have been successfully used for solid-state laser mode-locking [4]. In standard measurements of reflectivity as a function of fluence, the induced absorption following the induced transmission peak will appear as non-saturable losses. Indeed, such measurements showed that the non-saturable loss in the structure H was 2.06 % compared to 0.61 % in the structure F, which had the same

number of QD layers but substantially different of differential reflectivity dynamics as discussed above.

To examine the excess carrier dynamics, especially those in the QD states, time-resolved PL measurements were conducted. The PL set-up allows measurements on a longer timescale of up to 1.5 ns. Excitation occurred at photon energies larger than the GaAs barrier's gap energy, i.e., into the barriers and the QDs, with the barrier absorption prevailing. Figure 5 shows the resulting PL spectrograms for all of the samples. The PL at wavelengths longer than 1  $\mu\text{m}$  is attributed to the radiative recombination of QD states, while the PL at shorter wavelengths are related to the states in the wetting layer and are a reminder of the strong GaAs PL background leaking through the cut-on filter. The modulation of the PL from the WL is believed to be a result of cavity effects, i.e., the wavelength-dependent enhancement factor as well as the structures power reflectivity. The excitation fluence was 19  $\mu\text{J}/\text{cm}^2$  for all samples, but sample H, where the data from stronger excitation with 550  $\mu\text{J}/\text{cm}^2$  are shown, since the PL signal was rather weak. Integration of the QDs' luminescence spectra yields the relaxation traces shown in Fig. 6 for all of the samples and for different excitation intensities.

The ratio of the PL signals' maxima for excitation at 6.3 and 19  $\mu\text{J}/\text{cm}^2$  corresponds well to the ratio of these excitation fluences. For stronger excitation, the increase in

**Fig. 5** Time-resolved PL as a function of the wavelength for all four samples. A logarithmic scale was used for the PL intensity to increase the visibility of the luminescence from the barrier and the WL. Each data set is normalised to the peak PL signal. The contributions from the barrier, the WL and the QDs are marked by the *white arrows* in plot (a). The excitation fluence was  $19 \mu\text{J}/\text{cm}^2$  for all of the samples but sample *H*, for which the data from stronger excitation with  $550 \mu\text{J}/\text{cm}^2$  are shown. The noise level varies over the spectral range due to the different sensitivity settings used for recording of the data at different wavelength intervals

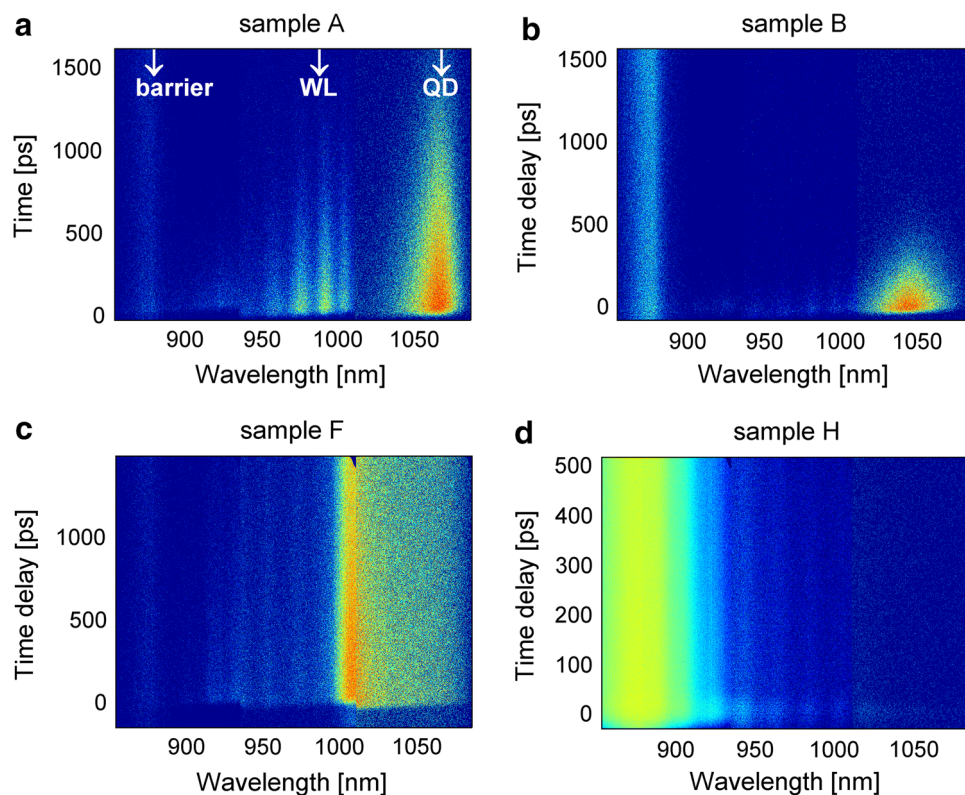
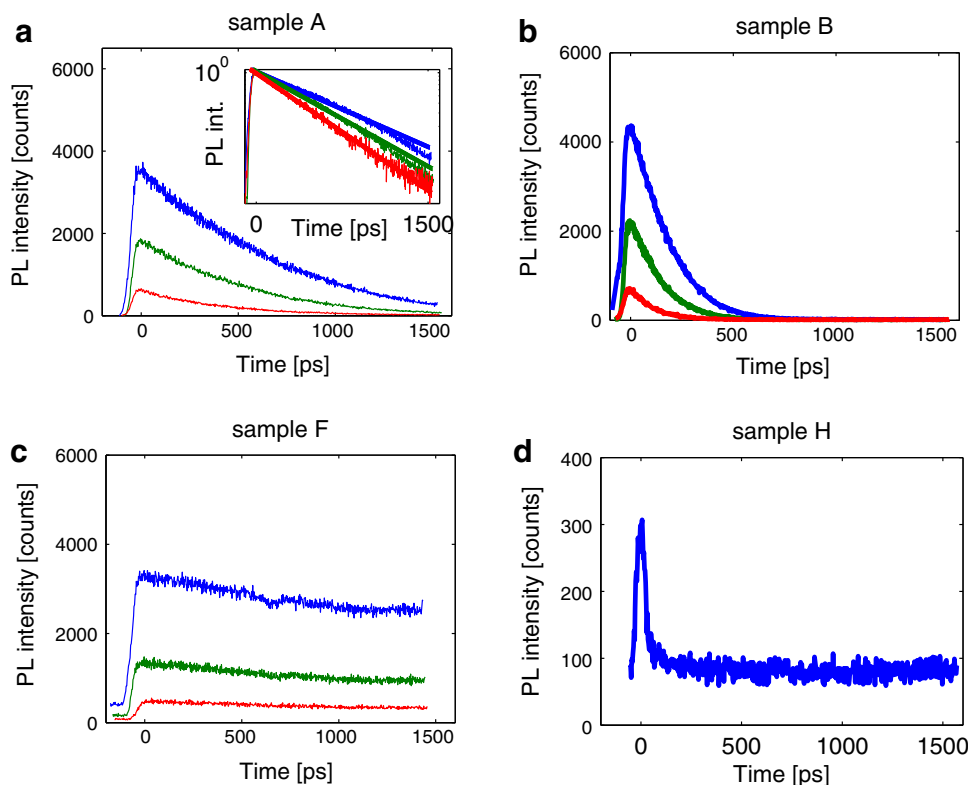


**Fig. 6** Transient behaviour on a longer timescale of up to 1.5 ns obtained by PL spectroscopy. The luminescence of the three samples **a** A, **b** B and **c** F was recorded for excitation fluences of  $57 \mu\text{J}/\text{cm}^2$  (blue curves),  $19 \mu\text{J}/\text{cm}^2$  (green curves) and  $6.3 \mu\text{J}/\text{cm}^2$  (red curves). The graph **d** for sample *H* was recorded for an excitation fluence of  $550 \mu\text{J}/\text{cm}^2$ . Note the different y axis scaling in graph **d** for sample *H*. The zero on the time axis is normalised to the PL signal's maximum. The *inset* in **a** shows the normalised PL signals from sample *A* on a logarithmic scale and an exponential fit for each data set



the PL intensity becomes sub-linear, indicating saturation of the QDs. This also follows from a rough estimate of the numbers of created carriers: assuming a GaAs volume of about  $1 \mu\text{m}$  length and an absorption coefficient on the order of  $1 \times 10^4 \text{ cm}^{-1}$  at 782 nm, about 73 % of the incident photons are absorbed. Given the excitation fluences, this yields  $1.8 \times 10^{13}$ – $1.6 \times 10^{14} \text{ cm}^{-2}$  absorbed photons as compared to a total QD density of about  $7.2 \times 10^{10} \text{ cm}^{-2}$  for sample A and  $6 \times 10^{10} \text{ cm}^{-2}$  for samples F and H. Even noting that, the number of electron states in an individual QD may be around ten (for three QD levels), the number of QD states is still much smaller than the number of pump photons. In this situation, the observed PL dynamics from the QD states is determined by the decay of the excess carrier concentration in quasi-continuum states either through radiative recombination in QDs or non-radiative recombination capture by defects and interface states. The resonance conditions of the structure also have a profound effect on the PL dynamics. In this respect, it is interesting to compare structures A and B. The PL decay time for sample A is determined by fitting a single exponential to the data, which yields 430, 530 and 670 ps for the increasing fluence. The fits are shown on a logarithmic scale in the inset of Fig. 6a. The agreement between data and single exponential fit is good for weak excitation, but starts to fail for stronger excitation due to the rather slow radiative decay via the QD states. The resonantly enhanced fluorescence field in the structure increases the effective relaxation time due to reabsorption in the QDs. It is clearly seen in Fig. 6b that the relaxation in the structure B, which is identical to A, except for the lower field enhancement factor, is substantially faster and corresponds to 124, 150 and 183 ps at the respective excitation fluences.

The resonant condition of the structure is not the only factor and not the main factor determining the PL decay, and, by extension, the decay of the long-living increased transmission in QD saturable absorber structures. It becomes obvious by comparing the PL dynamics in structures A and B with that of the structure F (Fig. 6c). The structure F is anti-resonant, with a six times smaller field enhancement factor than the structure B. The PL decay, however, is very slow indeed. The PL decay time for structure F is estimated by assuming a single exponential decay and assigning the background signal just before the excitation pulse to the residual PL excited by the previous pulse. Knowing the repetition rate of the excitation laser, a recombination time on the order of 7 ns can be estimated. To understand this, it should first be noted that the maximum number of PL photon counts in structures A, B and F is similar for the same excitation fluences, indicating that the concentrations of fast capture and non-radiative recombination centres as well as the density of

QDs is similar in these structures. On the other hand, the structure F has two times thicker GaAs spacer layers between the QD stacks, 20 nm compared to 10 nm, respectively. This provides a two times larger pool of excess carriers in the structure F, which will have to recombine radiatively through saturated QD states in the absence of a more efficient recombination channel.

The PL signal from the QDs in structure H even at excitation fluences of  $550 \mu\text{J}/\text{cm}^2$  is rather low and decays very fast, as shown in Fig. 6d. The PL transient duration is limited here by the resolution of the measurement set-up. Note that, the structure H is similar to the structure F with 20 nm-thick GaAs barriers and the same total number of QD layers, except that the QD layers are grouped in five in this structure. The low PL and the fast relaxation are indicators of a very efficient non-radiative relaxation channel and are in agreement with time-resolved differential reflectivity measurements, as was already argued above.

#### 4 Conclusions

We presented results from studying the carrier dynamics in self-assembled InAs/GaAs quantum-dot saturable absorbers intended for mode-locking of solid-state lasers operating around 1,040 nm. Four samples with controlled variations in design were examined. Specifically, the controlled parameters were the field enhancement factor related to the resonant condition of the absorber, the thickness of the GaAs barriers and the number of QD layers in the QD stacks positioned in the anti-nodes of the internal electric field distribution. Time-resolved differential reflectivity pump-probe experiments at a wide range of excitation fluences were conducted and revealed that at low excitation fluences, the initial bleaching of the absorption has a predominant fast relaxation component, while the slowly relaxing induced transparency rises and becomes dominant at higher excitation fluences. The TPA appearing in resonant and semi-resonant structures (A and B, respectively) might help stabilise mode-locked laser operation; however, one has to be aware of large and slowly relaxing induced transparency due to a capture of excess carriers from the barrier bands into the QDs and a slow radiative recombination there, as was revealed by time-resolved PL measurements. The PL measurements show that the field enhancement on resonance decreases this relaxation rate, which is detrimental for mode-locking applications. An even stronger effect in this sense has the increase in the barrier thickness between the QD stacks. In this case, even in non-resonant structures, the relaxation process takes several nanoseconds, in effect, limiting the applicability of such structures for lasers with pulse

repetition rates below 50 MHz. By far, the fastest response was obtained in a structure with the largest number of QD layers (5) per stack, which we attribute to the appearance of efficient non-radiative recombination channels and capture centres. These centres are probably related to dislocations and other defects appearing in thick QD stacks. Such QD saturable absorbers indeed show subpicosecond relaxation and were utilised in mode-locking high-repetition rate solid-state lasers. This conclusion should come with caution, however, that the electron or hole capture centres might be long living and appear as non-saturable loss, reducing the laser efficiency and possibly also reducing the damage threshold at higher repetition rates. Clearly, the recombination times could be reduced deliberately by other different means, e.g., proton bombardment, which has proven to be feasible for quantum wells [29] as well as QDs [30]. A reverse electric bias applied to a QD absorber in a p-i-n structure can also be an efficient way to remove an excess carrier concentration from GaAs barrier layers [18], [31], [32].

**Acknowledgments** This work was in part funded by the European Community FP7 FAST-DOT project under Grant Agreement 224668 and by the Swedish Research Council (VR) through its Linnæus Center of Excellence ADOPT.

## References

- N.N. Ledentsov, Quantum dot laser. *Semicond. Sci. Technol.* **26**(1), 014001 (2011)
- E.U. Rafailov, S.J. White, A.A. Lagatsky, A. Miller, W. Sibbett, D.A. Livshits, A.E. Zhukov, V.M. Ustinov, Fast quantum-dot saturable absorber for passive mode-locking of solid-state lasers. *IEEE Photonics Technol. Lett.* **16**(11), 2439–2441 (2004)
- D. Lorensen, H.J. Unold, D.J.H.C. Maas, A. Aschwanden, R. Grange, R. Paschotta, D. Ebling, E. Gini, U. Keller, Towards wafer-scale integration of high repetition rate passively mode-locked surface-emitting semiconductor lasers. *Appl Phys B* **79**(8), 927–932 (2004)
- N. Meiser, K. Seger, V. Pasiskevicius, H. Jang, E. Rafailov, I. Krestnikov, Gigahertz repetition rate mode-locked Yb:KYW laser using self-assembled quantum dot saturable absorber. *Appl. Phys. B* **110**(3), 327–333 (2013)
- A.A. Lagatsky, F.M. Bain, C.T.A. Brown, W. Sibbett, D.A. Livshits, G. Erbert, E.U. Rafailov, Low-loss quantum-dot-based saturable absorber for efficient femtosecond pulse generation. *Appl. Phys. Lett.* **91**, 231111 (2007)
- A.A. Lagatsky, F. Fusari, S. Calvez, J.A. Gupta, V.E. Kisel, N.V. Kuleshov, C.T.A. Brown, M.D. Dawson, W. Sibbett, Passive mode locking of a Tm, Ho:KY(WO<sub>4</sub>)<sub>2</sub> laser around 2  $\mu$ m. *Opt. Lett.* **34**(17), 2587–2589 (2009)
- V.G. Savitski, P.J. Schlosser, J.E. Hastie, A.B. Krysa, J.S. Roberts, M.D. Dawson, D. Burns, S. Calvez, Passive mode-locking of a Ti : sapphire laser by InGaP quantum-dot saturable absorber. *IEEE Photonics Technol. Lett.* **22**(4), 209–211 (2010)
- M. Hoffmann, O.D. Sieber, V.J. Wittwer, I.L. Krestnikov, D.A. Livshits, Y. Barbarin, T. Südmeyer, U. Keller, Femtosecond high-power quantum dot vertical external cavity surface emitting laser. *Opt. Express* **19**(9), 8108–8116 (2011)
- C. Hönninger, R. Paschotta, F. Morier-Genoud, M. Moser, U. Keller, Q-switching stability limits of continuous-wave passive mode locking. *J. Opt. Soc. Am. B* **16**(1), 46–56 (1999)
- U. Keller, Recent developments in compact ultrafast lasers. *Nature* **424**, 831–838 (2003)
- W. Yang, R.R. Lowe-Webb, H. Lee, P.C. Sercel, Effect of carrier emission and retrapping on luminescence time decays in InAs/GaAs quantum dots. *Phys. Rev. B* **56**(20), 13314–13320 (1997)
- R. Heitz, A. Kalburge, Q. Xie, M. Grundmann, P. Chen, A. Hoffmann, A. Madhukar, D. Bimberg, Excited states and energy relaxation in stacked InAs/GaAs quantum dots. *Phys. Rev. B* **57**(15), 9050–9060 (1998)
- T.S. Sosnowski, T.B. Norris, H. Jiang, J. Singh, K. Kamath, P. Bhattacharya, Rapid carrier relaxation in In<sub>0.4</sub>Ga<sub>0.6</sub>As/GaAs quantum dots characterized by differential transmission spectroscopy. *Phys. Rev. B* **57**(16), R9423–R9426 (1998)
- P. Borri, W. Langbein, J.M. Hvam, F. Heinrichsdorff, M.-H. Mao, D. Bimberg, Ultrafast gain dynamics in InAs-InGaAs quantum-dot amplifiers. *Photonics Technol. Lett. IEEE* **12**(6), 594–596 (2000)
- S. Raymond, K. Hinzer, S. Fafard, J.L. Merz, Experimental determination of Auger capture coefficients in self-assembled quantum dots. *Phys. Rev. B* **61**(24), R16331–R16334 (2000)
- H.P. Porte, P. Uhd Jepsen, N. Daghestani, E.U. Rafailov, D. Turchinovich, Ultrafast release and capture of carriers in InGaAs/GaAs quantum dots observed by time-resolved terahertz spectroscopy. *Appl. Phys. Lett.* **94**(26), 262104 (2009)
- R. Leon, S. Marcinkecius, J. Siegert, B. Cechavicius, B. Magness, W. Taylor, C. Lobo, Effects of proton irradiation on luminescence emission and carrier dynamics of self-assembled III-V quantum dots. *IEEE Trans. Nucl. Sci.* **49**(6), 2844–2851 (2002)
- X. Liu, E.U. Rafailov, D. Livshits, D. Turchinovich, Quantum well saturable absorber mirror with electrical control of modulation depth. *Appl. Phys. Lett.* **97**(5), 051103 (2010)
- A.-R. Bellancourt, Y. Barbarin, D.J.H.C. Mass, M. Shafiei, M. Hoffmann, M. Golling, T. Südmeyer, U. Keller, Low saturation fluence antiresonant quantumdot SESAMs for MIXSEL integration. *Opt. Express* **17**(12), 9704–9711 (2009)
- E.R. Thoen, E.M. Koontz, M. Joschko, P. Langlois, T.R. Schibli, F.X. Kärtner, E.P. Ippen, L.A. Kolodziejski, Two-photon absorption in semiconductor saturable absorber mirrors. *Appl. Phys. Lett.* **74**(26), 3927–3929 (1999)
- P. Langlois, M. Joschko, E.R. Thoen, E.M. Koontz, F.X. Kärtner, E.P. Ippen, L.A. Kolodziejski, High fluence ultrafast dynamics of semiconductor saturable absorber mirrors. *Appl. Phys. Lett.* **75**, 3841 (1999)
- R. Grange, M. Haiml, R. Paschotta, G.J. Spühler, L. Krainer, M. Golling, O. Ostinelli, U. Keller, New regime of inverse saturable absorption for self-stabilizing passively mode-locked lasers. *Appl. Phys. B: Lasers Opt.* **80**, 151–158 (2005)
- M. Joschko, P. Langlois, E.R. Thoen, E.M. Koontz, E.P. Ippen, L.A. Kolodziejski, Ultrafast hot-carrier dynamics in semiconductor saturable absorber mirrors. *Appl. Phys. Lett.* **76**(11), 1383–1385 (2000)
- F. Schättiger, D. Bauer, J. Demsar, T. Dekorsy, J. Kleinbauer, D.H. Sutter, J. Puustinen, M. Guina, Characterization of InGaAs and InGaAsN semiconductor saturable absorber mirrors for high-power mode-locked thin-disk lasers. *Appl. Phys. B* **106**(3), 605–612 (2012)
- Q. Li, Z.Y. Xu, W.K. Ge, Carrier capture into InAs/GaAs quantum dots detected by a simple degenerate pump-probe technique. *Solid State Commun.* **115**(2), 105–108 (2000)
- D. Maas, A. Bellancourt, M. Hoffmann, B. Rudin, Y. Barbarin, M. Golling, T. Südmeyer, U. Keller, Growth parameter optimization for fast quantum dot SESAMs. *Opt. Express* **16**(23), 18646–18656 (2008)



27. J.T. Ng, U. Bangert, M. Missous, Formation and role of defects in stacked large binary InAs/GaAs quantum dot structures. *Semicond. Sci. Technol.* **22**(2), 80 (2007)
28. D. Alonso-Alvarez, A.G. Taboada, J.M. Ripalda, B. Alen, Y. Gonzalez, L. Gonzalez, J.M. Garcia, F. Briones, A. Marti, A. Luque, A.M. Sanchez, S.I. Molina, Carrier recombination effects in strain compensated quantum dot stacks embedded in solar cells. *Appl. Phys. Lett.* **93**(12), 123114 (2008)
29. Y. Silberberg, P.W. Smith, D.A.B. Miller, B. Tell, A.C. Gossard, W. Wiegmann, Fast nonlinear optical response from proton-bombarded multiple quantum well structures. *Appl. Phys. Lett.* **46**(8), 701–703 (1985)
30. S. Marcinkevičius, J. Siegert, R. Leon, B. Čechavičius, B. Magness, W. Taylor, C. Lobo, Changes in luminescence intensities and carrier dynamics induced by proton irradiation in  $\text{In}_x\text{Ga}_{1-x}\text{As}/\text{GaAs}$  quantum dots. *Phys. Rev. B* **66**(23), 235314 (2002)
31. A.A. Lagatsky, E.U. Rafailov, W. Sibbett, D.A. Livshits, A.E. Zhukov, V.M. Ustinov, *Quantum-dot based saturable absorber with p-n junction for mode locking of solid-state lasers*, Conference on Lasers and Electro-Optics/International Quantum Electronics Conference and Photonic Applications Systems Technologies, vol. (2004) p. CThV6
32. S.A. Zolotovskaya, M. Butkus, R. Häring, A. Able, W. Kaenders, I.L. Krestnikov, D.A. Livshits, E.U. Rafailov, p-i-n junction quantum dot saturable absorber mirror: electrical control of ultrafast dynamics. *Opt. Express* **20**(8), 9038–9045 (2012)